

## Fractional Topological States of Dipolar Fermions in One-Dimensional Optical Superlattices

Zhihao Xu, Linhu Li, and Shu Chen\*

*Beijing National Laboratory for Condensed Matter Physics, Institute of Physics,  
Chinese Academy of Sciences, Beijing 100190, China  
(Received 8 November 2012; published 21 May 2013)*

We study the properties of dipolar fermions trapped in one-dimensional bichromatic optical lattices and show the existence of fractional topological states in the presence of strong dipole-dipole interactions. We find some interesting connections between fractional topological states in one-dimensional superlattices and the fractional quantum Hall states: (i) the one-dimensional fractional topological states for systems at filling factor  $\nu = 1/p$  have  $p$ -fold degeneracy, (ii) the quasihole excitations fulfill the same counting rule as that of fractional quantum Hall states, and (iii) the total Chern number of  $p$ -fold degenerate states is a nonzero integer. The existence of crystalline order in our system is also consistent with the thin-torus limit of the fractional quantum Hall state on a torus. The possible experimental realization in cold atomic systems offers a new platform for the study of fractional topological phases in one-dimensional superlattice systems.

DOI: [10.1103/PhysRevLett.110.215301](https://doi.org/10.1103/PhysRevLett.110.215301)

PACS numbers: 67.85.-d, 03.75.Hh, 05.30.Fk, 73.21.Cd

*Introduction.*—Fractional quantum Hall (FQH) effects have attracted intensive studies in the past decades as an important subject in condensed matter physics. The traditional FQH states were realized in two-dimensional (2D) electron gases within a strong external magnetic field. In addition to 2D electron gases, great effort has been made to study quantum Hall effects in some other physical systems, for example, lattice systems without a magnetic field and cold atomic systems. Effective Landau levels can be realized in cold atomic systems in the presence of a rapidly rotating trap [1,2] or a laser-induced gauge field [3]. Because of the existence of long-range interaction, the dipolar Fermi gas is a good candidate to realize FQH states. The FQH effects in a 2D dipolar Fermi gas with either isotropic [4] or anisotropic dipole-dipole interaction (DDI) [5] have been studied recently.

As most of the previous studies on topological nontrivial states focus on 2D systems [6–8], the one-dimensional (1D) systems attracted less attention until very recently [9–11]. Although 1D systems without any symmetry are generally topologically trivial, the 1D superlattice model was recently found to be topologically nontrivial [9,10] as the periodic parameter in these superlattice models can be considered as an additional dimension and thus the systems may have a nontrivial Chern number in an effective 2D parameter space. It has been shown that the 1D superlattice system with subbands being filled is not a trivial band insulator but a topological insulator with a nonzero Chern number [9], which can be viewed as a correspondence of the integer quantum Hall state of a 2D square lattice [12,13] in the reduced 1D system. It is well known that the FQH effect emerges from the integer quantum Hall state in the presence of strong long-range interactions. It is natural to ask whether a fractional topological state is

available for the 1D superlattice system when interactions are included.

In this Letter, we explore the nontrivial topological properties of dipolar fermions in 1D bichromatic optical lattices, which can be realized in cold atom experiments by loading the dipolar fermions into the lattice superposed by two 1D optical lattices with different wavelengths [14,15]. The noninteracting part of our Hamiltonian is the recently studied 1D superlattice model with topologically nontrivial bands [9,10]. The presence of dipolar interactions breaks down the band description within a noninteracting picture. To characterize topological features of the interacting system, we study the low-energy spectrum and the topological Chern number of the dipolar system based on exact calculation of finite-size systems. The existence of nontrivial topological states for the strongly interacting system at fractional filling is demonstrated by the topological degeneracy and nontrivial Chern number of the low-energy states. Particularly, recent progress in manipulating ultracold polar molecules [16] offers the possibility of exploring exotic quantum states of Fermi gases with strong dipolar interactions in the topologically nontrivial optical lattices.

*Model Hamiltonian.*—We consider a 1D Fermi gas with DDIs in a bichromatic optical superlattice:

$$H = -t \sum_i (c_i^\dagger c_{i+1} + \text{H.c.}) + \sum_i \mu_i n_i + \frac{V}{2} \sum_{i \neq j} \frac{n_i n_j}{|i-j|^3}, \quad (1)$$

with

$$\mu_i = \lambda \cos(2\pi\alpha i + \delta), \quad (2)$$

where  $c_i^\dagger$  ( $c_i$ ) is the creation (annihilation) operator of fermions,  $n_i = c_i^\dagger c_i$  the density operator, and  $t$  the hopping

strength. Here  $\mu_i$  is the periodic potential with  $\lambda$  being the modulation amplitude,  $\alpha$  determining the modulation period, and  $\delta$  being an arbitrary phase. The last term of Eq. (1) is for DDIs which are long-range interactions decayed with  $1/r^3$  with  $V$  the strength of DDI. For convenience, we shall set  $t = 1$  as the unit of energy and choose  $\alpha = 1/q$ .

In the absence of interactions, it has been demonstrated that the system with its subbands fully filled by fermions is an insulator with a nontrivial topological Chern number in a 2D parameter space spanned by momentum and the phase of  $\delta$  [9]. If the subband is only partially filled, the system is a topologically trivial conductor. In this Letter, we shall study the case with the lowest band being partially filled by fermions subjected to the long-range interaction. Given that the number of fermions is  $N$  and the lattice size is  $L$ , the filling factor is defined as  $\nu = N/N_{\text{cell}}$  with  $N_{\text{cell}} = L/q$  being the number of primitive cells. While  $\nu = 1$  corresponds to the lowest band being fully filled, in this Letter we shall consider the system with a fractional filling factor, for example,  $\nu = 1/3$  and  $\nu = 1/5$ .

*Low-energy spectrum and ground state degeneracy.*—In the presence of the long-range DDI term, we diagonalize the Hamiltonian (1) in each momentum subspace with  $k = 2\pi m/N_{\text{cell}}$  under the periodic boundary condition (PBC) [17], where  $m$  takes  $0, 1, \dots, N_{\text{cell}} - 1$ . For finite-size systems with a given fractional filling, we study the change of low-energy spectrum with the increase in the interaction strength  $V$ . In Fig. 1, we display the low-energy spectrum in momentum sectors for systems with  $t = 1$ ,  $\nu = 1/3$ ,  $\lambda = 1.5$ ,  $\alpha = 1/3$ ,  $\delta = 5\pi/4$ , and different  $V$ . Various cases with particle numbers  $N = 2, 3, 4$  are shown in the same figure. When  $V$  is small, it is hard to distinguish the lowest states from the higher excited states by an obvious gap. When  $V$  exceeds 50, the lowest three states

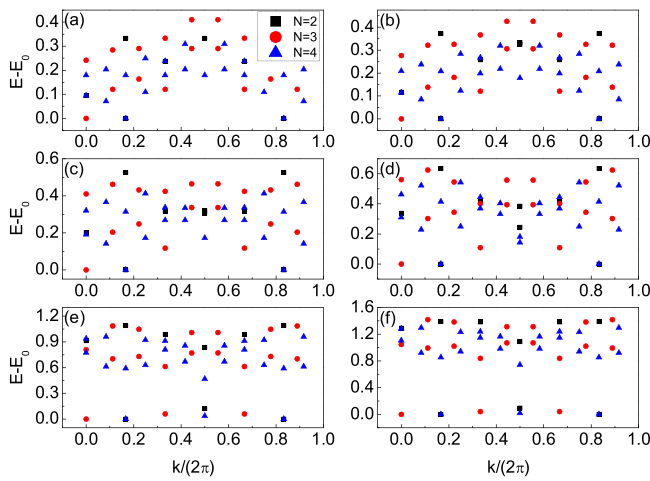


FIG. 1 (color online). Low-energy spectrum in momentum space with filling factor  $\nu = 1/3$ ,  $t = 1$ ,  $\lambda = 1.5$ ,  $\alpha = 1/3$ ,  $\delta = 5\pi/4$ , and different  $V$  under the PBC. (a)–(f)  $V$  takes 0, 1, 10, 50, 300, and 500, respectively.

tend to form a ground-state (GS) manifold with an obvious gap separating them from higher ones. As  $V$  increases further, the gap becomes more obvious and the lowest three states become nearly degenerate at  $V = 500$ . The threefold degeneracy does not depend on particle numbers, but is only relevant to the filling factor  $\nu = 1/3$ .

In the large  $V$  case, the lowest three states in the GS manifold always appear at some determinate positions in the momentum space. For cases of  $N = 2, 4$  (even), the total momenta locate at  $K = \pi/3, \pi, 5\pi/3$ , whereas for  $N = 3$  (odd), at  $K = 0, 2\pi/3, 4\pi/3$ . We observe that one can make a connection between the momenta in our system and the orbital momenta of the FQH system in the thin-torus limit by setting  $N_\phi = N_{\text{cell}}$  with  $N_\phi$  being the number of the flux quanta. According to the exclusion rule known from the thin-torus limit of the FQH system [18,19], the total momenta of the  $p$ -fold degenerate GSs emerge at  $K = (2\pi)\{[pN(N-1)/2 + lN] \bmod N_{\text{cell}}\}/N_{\text{cell}}$ , where  $l = 0, 1, \dots, p-1$  for a system with  $\nu = 1/p$ . We also check the low-energy spectra for systems with  $t = 1$ ,  $\nu = 1/5$ ,  $\lambda = 1.5$ ,  $\alpha = 1/3$ ,  $\delta = 5\pi/4$ , and different  $V$ . Similar to cases of  $\nu = 1/3$ , both systems with  $N = 2$  and  $N = 3$  show the fivefold degenerate GS manifold in the large  $V$  limit and the positions of momenta fulfill the above expression determined by the exclusion rule.

*Quasihole excitation spectrum.*—For FQH states, the existence of quasihole excitations, which fulfill fractional statistics [20,21], is an important characteristic feature of the system. According to the general counting rule [18], the number of quasiholes for the FQH system of  $\nu = 1/3$  reads as  $N_{qh} = N_{\text{cell}} \frac{(N_{\text{cell}} - 2N - 1)!}{N!(N_{\text{cell}} - 3N)!}$ . Next we study the quasihole excitations by removing a particle from our system and check whether a similarity to the FQH system exists. On the left part of Fig. 2, we show the quasihole excitation

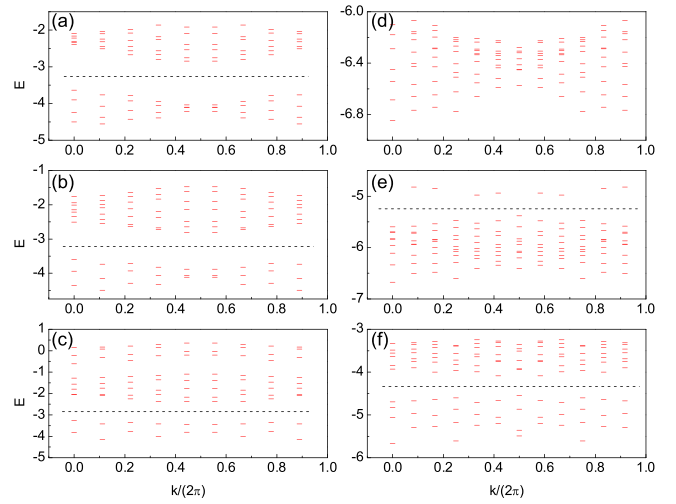


FIG. 2 (color online). Quasihole excitation spectrum. The left part is for the system with  $N = 2$ ,  $L = 27$ , and  $V = 1, 50, 500$  from top to bottom. The right part is for  $N = 3$ ,  $L = 36$ , and  $V = 1, 50, 500$  from top to down.

spectra for the system with  $N = 2$  and  $L = 27$  produced by removing a particle from the system of  $\nu = 1/3$  with  $N = 3$  and  $L = 27$ , whereas the right part of Fig. 2 gives spectra for  $N = 3$  and  $L = 36$  by removing a particle from the system of  $\nu = 1/3$  with  $N = 4$  and  $L = 36$ . For both parts, from top to bottom  $V = 1, 50$ , and  $500$ , respectively. In the regime of small  $V$ , the number of quasihole excitations is much larger than that given according to the above accounting rule of FQH systems. As  $V$  increases, the low-energy parts are excited into the upper part. For  $V = 500$ , as shown in Fig. 2(c), below the gap, the number of quasihole excitations is 18 with two states on each momentum sector. In Fig. 2(f), the total number of states under the dash line is 40 and for momentum sectors  $[kN_{\text{cell}}/(2\pi)] \bmod 3 = 0$ , the number of states below the gap is four while in the other parts is three, due to the finite-size effect. For both cases with  $V = 500$ , the total number of states below the gap is consistent with the number obtained by the counting rule for the  $\nu = 1/3$  FQH state.

*Topological feature of ground-state manifold.*—To characterize the topological feature of the many-body states, we introduce the twist boundary condition  $\psi(r + L, \delta) = e^{i\theta} \psi(r, \delta)$ , where  $\theta$  is the introduced phase factor. Under the twist boundary condition, the momentum  $k$  in Brillouin zone gets a shift  $k = (2\pi m + \theta)/N_{\text{cell}}$  with  $m = 0, 1, \dots, N_{\text{cell}} - 1$ . Correspondingly, the energies vary continuously with the change of  $\theta$ . In Fig. 3, we show the low energy spectra as a function of  $\theta$  (the spectrum flux) at a fixed  $\delta = 5\pi/4$  for systems with  $N = 2$  [(a)–(c)] and  $N = 3$  [(d)–(f)]. In the small  $V$  regime of  $V = 1$ , the lower energy levels overlap together with the change of  $\theta$ . For  $V = 50$ , the lowest three energy spectra flow into each other but are already separated from the higher states. For  $V = 500$ , the lowest three states are nearly degenerate,

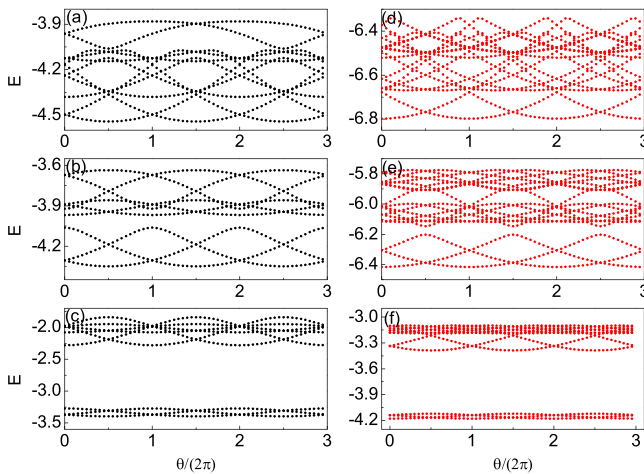


FIG. 3 (color online). Spectrum flux versus  $\theta$  for systems with  $t = 1$ ,  $\nu = 1/3$ ,  $\lambda = 1.5$ ,  $\alpha = 1/3$ ,  $\delta = 5\pi/4$ , and different  $V$ . (a)–(c)  $N = 2$ ,  $V = 1, 50$ , and  $500$ , respectively. (d)–(f)  $N = 3$ ,  $V = 1, 50$ , and  $500$ , respectively.

and the GS manifold is well separated from the higher states by a gap. Similarly, if the phase  $\delta$  varies from  $0$  to  $2\pi$ , the spectrum for a given  $\theta$  changes continuously with the GS manifold well separated from the other states, which indicates the robustness of GS manifold in the large  $V$  regime. An example for  $\theta = 0$  corresponding to the PBC is given in Fig. 4(a).

In the 2D parameter space of  $(\theta, \delta)$ , the Chern number of the many-body state is defined as an integral invariant  $C = \frac{1}{2\pi} \int d\theta d\delta F(\theta, \delta)$ , where  $F(\theta, \delta) = \text{Im}(\langle \frac{\partial \psi}{\partial \delta} | \frac{\partial \psi}{\partial \theta} \rangle - \langle \frac{\partial \psi}{\partial \theta} | \frac{\partial \psi}{\partial \delta} \rangle)$  is the Berry curvature [12,22]. Considering the system with  $V = 500$  shown in Fig. 1(f), we calculate the Chern numbers of the lowest three nearly degenerate states in the GS manifold. For a system of  $N = 2$ , the Chern numbers of the three states are  $C_1 = 0.4036$ ,  $C_2 = 0.1928$ , and  $C_3 = 0.4036$ , respectively. For each state, the Chern number is not an integer, but their sum is an integer  $\sum_{i=1}^3 C_i = 1$ . Similarly, for  $N = 3$ , we have  $C_1 = 0.2776$ ,  $C_2 = 0.4448$ , and  $C_3 = 0.2776$  with their summation being 1. The existence of a nonzero total Chern number characterizes the system at fractional filling having nontrivial topological properties. Effectively, the total Chern number is shared by the  $q$  degenerate states, which is similar to the FQH system with its  $q$ -fold GSs sharing an integer total Chern number [23].

The emergence of edge states under the open boundary condition (OBC) is generally characteristic of topologically nontrivial phases. In Fig. 4(b), we show the low-energy spectra as a function of phase  $\delta$  under the OBC, which is obtained by setting the hopping amplitude between the first and  $L$ th site as zero. In contrast to the spectra under the PBC, inside the gap regime, there emerge

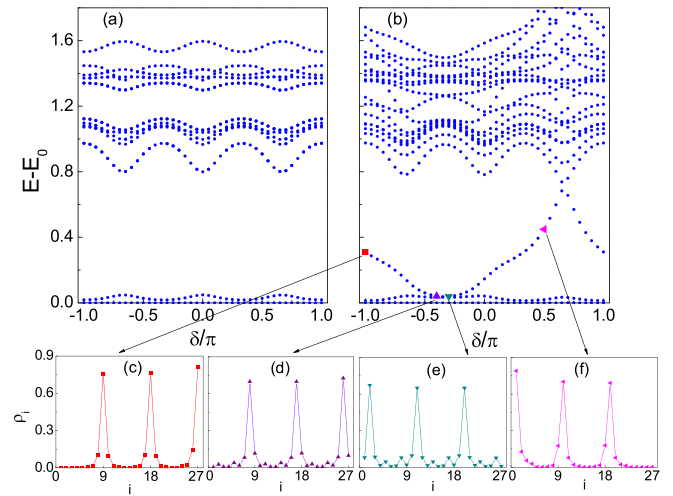


FIG. 4 (color online). The low energy spectrum as the function of the phase  $\delta$  for the system with  $L = 27$ ,  $N = 3$ ,  $t = 1$ ,  $\lambda = 1.5$ ,  $\alpha = 1/3$ ,  $V = 500$ . Here  $E_0$  represents the GS energy of the system. (a) is for the PBC; (b) is for the OBC; (c)–(f) is the density distribution for the in-gap mode with  $\delta = -\pi, -0.4\pi, -0.3\pi$ , and  $0.5\pi$ , respectively.

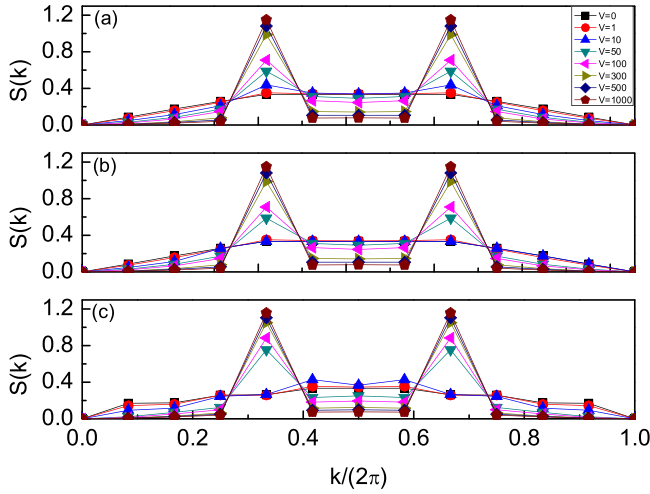


FIG. 5 (color online). Static structure factor  $S(k)$  of the lowest three energy states versus momentum  $k$  for the system with different  $V$ . Here,  $N = 4$ ,  $L = 36$ .

edge modes which connect the GS and excitation branch of the bulk spectrum as one varies phase  $\delta$ . As shown in Figs. 4(c)–4(f), the state is adiabatically changed with  $\delta$  varying from  $-\pi$  to  $\pi/2$ . The density distribution  $\rho_i$  shows that the in-gap state with  $\delta = -\pi$  is pinned down on the right edge, whereas the state with  $\delta = \pi/2$  is pinned down on the left edge.

The density distributions shown in Figs. 4(c)–4(f) already display the signature of a crystallized phase. To reveal the crystalline character of systems with the PBC, we introduce the static structure factor  $S(k)$  defined as

$$S(k) = \frac{1}{N_{\text{cell}}} \sum_{i,j} e^{ik(i-j)} [\langle n_i^c n_j^c \rangle - \langle n_i^c \rangle \langle n_j^c \rangle], \quad (3)$$

where  $n_i^c = n_{qi} + n_{qi+1} + \dots + n_{qi+q-1}$  is the sum of the particle number operators in the  $i$ th primitive cell and  $i = 0, 1, \dots, N_{\text{cell}} - 1$ . Figure 5 shows the static structure factor of the three lowest eigenstates versus momentum for the system with  $N = 4$ ,  $L = 36$ , and different  $V$ . In the strong repulsive limit, peaks emerge at  $k = 2\pi/3, 4\pi/3$  for all the lowest three eigenstates. With the increase of  $V$ , the height of the peaks increases and the central parts of the  $S(k)$  decrease dramatically, which suggests that these states are crystallized with a periodic structure in the large  $V$  limit. The existence of topologically nontrivial crystallized phase in our system is consistent with previous works on the evolution of FQH states on a torus [24–26], which have shown that the FQH state on a torus is adiabatically connected to a crystallized phase as the 2D system is deformed to the 1D thin-torus limit.

The emergence of fractional topological states is a consequence of interplay of nontrivial topology of superlattices and long-range interactions, which is illustrated by the shift of edge mode from one to the other edge driven by the phase  $\delta$ . While the long-range interaction is responsible for

the formation of degenerate GS manifold, the nontrivial topology of superlattices guarantees the existence of edge states. Consequently, when the PBC is changed to the OBC, the threefold degenerate GSs are lifted and one of them develops into the edge mode as shown in Fig. 4(b). This is quite different from the noninteracting case, for which the GS is nondegenerate and nontrivial edge states only appear at the integer filling. To see clearly the effect of long-range interaction, we also check cases with the Coulomb interaction and short-range interactions [17]. While our conclusions also hold true for the case with Coulomb interaction, no degenerate GS manifold and fractional topological states are found for the case with short-range interactions even in the strongly interacting limit.

In summary, we demonstrate the existence of fractional topological states for dipolar fermions in topologically nontrivial 1D superlattices, which are characterized by the GS degeneracy, nontrivial total Chern number of GSs, and quasihole excitations fulfilling the same counting rule as the FQH states. The existence of crystallized order in the 1D fractional topological phases is also identified by calculating the structure factor. Our study provides a way of creating nontrivial fractional topological states by trapping the dipolar fermions in 1D bichromatic optical lattices which are realizable in current cold atomic experiments.

We thank X. Wan and Z. Liu for helpful discussions. This work has been supported by the National Program for Basic Research of MOST, the NSF of China under Grants No. 11174360 and No. 11121063, and 973 grant.

\*schen@aphy.iphy.ac.cn

- [1] N.R. Cooper, *Adv. Phys.* **57**, 539 (2008).
- [2] A.L. Fetter, *Rev. Mod. Phys.* **81**, 647 (2009).
- [3] Y.-J. Lin, R.L. Compton, K. Jimnez-Garcia, J.V. Porto, and I.B. Spielman, *Nature (London)* **462**, 628 (2009).
- [4] K. Osterloh, N. Barberán, and M. Lewenstein, *Phys. Rev. Lett.* **99**, 160403 (2007).
- [5] R.-Z. Qiu, F.D.M. Haldane, X. Wan, K. Yang, and S. Yi, *Phys. Rev. B* **85**, 115308 (2012); R.-Z. Qiu, S.-P. Kou, Z.-X. Hu, Xin Wan, and S. Yi, *Phys. Rev. A* **83**, 063633 (2011).
- [6] K. Osterloh, M. Baig, L. Santos, P. Zoller, and M. Lewenstein, *Phys. Rev. Lett.* **95**, 010403 (2005).
- [7] L.B. Shao, S.-L. Zhu, L. Sheng, D.Y. Xing, and Z.D. Wang, *Phys. Rev. Lett.* **101**, 246810 (2008).
- [8] M.Z. Hasan and C.L. Kane, *Rev. Mod. Phys.* **82**, 3045 (2010); X.-L. Qi and S.-C. Zhang, *Rev. Mod. Phys.* **83**, 1057 (2011).
- [9] L.-J. Lang, X.M. Cai, and S. Chen, *Phys. Rev. Lett.* **108**, 220401 (2012).
- [10] Y.E. Kraus, Y. Lahini, Z. Ringel, M. Verbin, and O. Zeitlinger, *Phys. Rev. Lett.* **109**, 106402 (2012).
- [11] F. Mei, S.L. Zhu, Z.M. Zhang, C.H. Oh, and N. Goldman, *Phys. Rev. A* **85**, 013638 (2012).

- [12] D.J. Thouless, M. Kohmoto, M.P. Nightingale, and M. den Nijs, *Phys. Rev. Lett.* **49**, 405 (1982).
- [13] D.R. Hofstadter, *Phys. Rev. B* **14**, 2239 (1976).
- [14] L. Fallani, J. E. Lye, V. Guarrera, C. Fort, and M. Inguscio, *Phys. Rev. Lett.* **98**, 130404 (2007).
- [15] G. Roati, C. D’Errico, L. Fallani, M. Fattori, C. Fort, M. Zaccanti, G. Modugno, M. Modugno, and M. Inguscio, *Nature (London)* **453**, 895 (2008); B. Deissler, M. Zaccanti, G. Roati, C. D’Errico, M. Fattori, M. Modugno, G. Modugno, and M. Inguscio, *Nat. Phys.* **6**, 354 (2010).
- [16] K.-K. Ni, S. Ospelkaus, M. H. G. de Miranda, A. Pe’er, B. Neyenhuis, J.J. Zirbel, S. Kotochigova, P.S. Julienne, D.S. Jin, and J. Ye, *Science* **322**, 231 (2008); S. Ospelkaus, A. Pe’er, K.-K. Ni, J.J. Zirbel, B. Neyenhuis, S. Kotochigova, P.S. Julienne, J. Ye, and D.S. Jin, *Nat. Phys.* **4**, 622 (2008).
- [17] See Supplemental Material at <http://link.aps.org/supplemental/10.1103/PhysRevLett.110.215301> for the low-energy spectra and discussions for cases with the Coulomb interaction and short-range interactions.
- [18] N. Regnault and B. A. Bernevig, *Phys. Rev. X* **1**, 021014 (2011).
- [19] E.J. Bergholtz and A. Karlhede, *Phys. Rev. B* **77**, 155308 (2008).
- [20] R. B. Laughlin, *Phys. Rev. Lett.* **50**, 1395 (1983).
- [21] B.I. Halperin, *Phys. Rev. Lett.* **52**, 1583 (1984); D. Arovas, J.R. Schrieffer, and F. Wilczek, *Phys. Rev. Lett.* **53**, 722 (1984).
- [22] Q. Niu, D.J. Thouless, and Y.S. Wu, *Phys. Rev. B* **31**, 3372 (1985).
- [23] D.N. Sheng, Z.C. Gu, K. Sun, and L. Sheng, *Nat. Commun.* **2**, 389 (2011).
- [24] A. Seidel, H. Fu, D.-H. Lee, J.M. Leinaas, and J. Moore, *Phys. Rev. Lett.* **95**, 266405 (2005).
- [25] E.J. Bergholtz and A. Karlhede, *Phys. Rev. Lett.* **94**, 026802 (2005).
- [26] E.J. Bergholtz and A. Karlhede, *J. Stat. Mech.* (2006) L04001; A. Seidel and D.-H. Lee, *Phys. Rev. Lett.* **97**, 056804 (2006).